Emergent SO(5) symmetry at the columnar ordering transition in the classical cubic dimer model

G. J. Sreejith,[1] Stephen Powell,[2] and Adam Nahum[3]

[1]*Indian Insitute for Science Education and Research, Pune 411008, India*
[2]*School of Physics and Astronomy, The University of Nottingham, Nottingham, NG7 2RD, United Kingdom*
[3]*Theoretical Physics, Oxford University, 1 Keble Road, Oxford OX1 3NP, United Kingdom*

The classical cubic-lattice dimer model undergoes an unconventional transition between a columnar crystal and a dimer liquid, in the same universality class as the deconfined quantum critical point in spin-1/2 antiferromagnets but with very different microscopic physics and microscopic symmetries. Using Monte Carlo simulations, we show that this transition has emergent SO(5) symmetry relating quantities characterizing the two phases. While the low-temperature phase has a conventional order parameter, the defining property of the Coulomb liquid on the high-temperature side is deconfinement of monomers, and so SO(5) relates fundamentally different types of objects. Studying linear system sizes up to $L = 96$, we find that this symmetry applies with an excellent precision, consistently improving with system size over this range. It is remarkable that SO(5) emerges in a system as basic as the cubic dimer model, with only simple discrete degrees of freedom. Our results are important evidence for the generality of the SO(5) symmetry that has been proposed for the NCCP^1 field theory. We describe an interpretation for these results in terms of a consistent hypothesis for the renormalization-group flow structure, allowing for the possibility that SO(5) may ultimately be a near-symmetry rather than exact.

The classical dimer model on the cubic lattice illustrates three key mechanisms in three-dimensional (3D) critical phenomena. Two of these are the appearance of artificial gauge fields, and unconventional phase transitions where topological effects play a key role. The third, which we demonstrate here, is the emergence in the infrared (IR) of unusual non-abelian symmetries that would be impossible at a conventional Wilson–Fisher-like critical point.

The close-packed dimer model has a power-law correlated 'Coulomb' phase [1, 2], governed by an emergent U(1) gauge field whose conserved flux arises from a 'magnetic field' defined in terms of dimers. A remarkable phase transition [3] separates this liquid from a 'columnar' phase, illustrated in Fig. 1(a), in which the dimers form a crystal, spontaneously breaking lattice symmetries. Despite being entirely classical, this transition is not described by Ginzburg–Landau theory, but is instead a Higgs transition of the U(1) gauge theory [4–6]. The effective field theory is the noncompact CP^1 model (NCCP^1), in which the gauge field couples to a two-component bosonic matter field that condenses at the transition.

NCCP^1 is also the effective field theory for the 'deconfined' Néel–valence-bond solid (VBS) phase transition [7, 8] in 2+1D quantum antiferromagnets [9–18] and a related lattice loop model [19]. This raises the possibility that the dimer model exhibits a surprising emergent symmetry: Simulations of the loop model show SO(5) symmetry emerging at large scales [20]—either exactly or to an extremely good approximation. Earlier work on topological sigma models for deconfined critical points [21, 22] revealed that SO(5) is a consistent possibility in the IR, despite the fact that it cannot be made manifest in the gauge theory [38]. The Néel–VBS transition involves a three-component antiferromagnetic order parameter and a two-component VBS order parameter; SO(5) allows all five components to be rotated into each other. This symmetry can be understood through a set of dualities for NCCP^1 and related theories [23].

Here we use Monte Carlo simulations to demonstrate emergent SO(5) at the dimer ordering transition. This large symmetry is particularly striking in a discrete classical model with no internal symmetries at all, only spatial symmetries together with a local constraint that is equivalent to U(1) symmetry in a dual representation. SO(5) furthermore unifies operators of conceptually distinct types, rotating the crystal order parameter—a conventional observable in terms of dimers—into 'monopole' operators that insert or remove monomers, and cannot be measured in the ensemble of dimer configurations. Together these yield a five-component SO(5) superspin. The emergent symmetry group is therefore identical to that of the Néel–VBS transition. But it should be noted that the *microscopic* symmetries of the latter—roughly speaking, SO(3) × (lattice symmetries)—are very different from the (lattice symmetries) × U(1) in the dimer model.

Previously, SO(5) has been demonstrated directly only in a single lattice model [20], and is also supported by level degeneracies in the JQ model [24], both realizations of the Néel–VBS transition. Its presence in the dimer model is particularly important because the IR behaviour of NCCP^1 is subtle and remains controversial [11, 12, 15–19, 23, 25–27]. The simplest explanation for SO(5) would be flow to a fixed point where

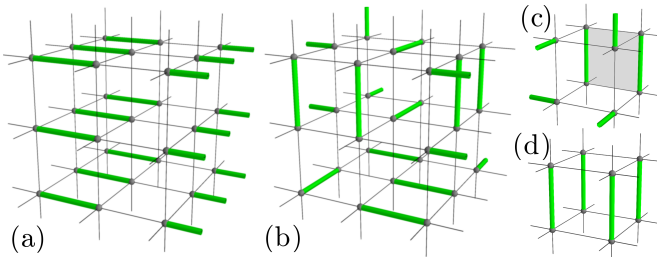

FIG. 1. Dimer model phases and interactions. (a) Columnar phase (one of six symmetry-related ground states). (b) Disordered configuration, typical of high-temperature Coulomb phase. (c) Pairs of nearest-neighbor parallel dimers (back face of cube) contribute energy $-v_2$. (d) Four parallel dimers around a cube contribute v_4.

allowed SO(5)-breaking perturbations are irrelevant, but there are reasons to doubt this occurs [23]. The transition may ultimately be first-order, with an exceptionally large but finite correlation length. However, even in the absence of a true continuous transition, the RG flows for NCCP^1 may ensure 'quasiuniversality' relating these transitions [19, 23], and approximate SO(5). In this scenario SO(5), though not exact, can hold to higher accuracy than standard finite-size scaling.

Given this complexity, it is important to test the robustness of SO(5). Finding SO(5) in the dimer model provides crucial confirmation that this is a generic property of models coarse-graining to NCCP^1, rather than one requiring further fine-tuning. The most striking feature of our results is that at length scales accessible numerically (up to linear size $L = 96$), SO(5) is indistinguishable from an exact symmetry of the IR theory.

Dimer model The degrees of freedom in this classical statistical model are dimers on the links of a cubic lattice, illustrated in Fig. 1. Defining the occupation number $d_\mu(\vec{r}) \in \{0, 1\}$ on the link joining site $\vec{r}$ to its neighbor $\vec{r} + \vec{\delta}_\mu$ ($\vec{\delta}_\mu$ is a unit vector), the number of dimers at site $\vec{r}$ is $n(\vec{r}) = \sum_\mu [d_\mu(\vec{r}) + d_\mu(\vec{r} - \vec{\delta}_\mu)]$. Close-packed dimer configurations are those where $n(\vec{r}) = 1$ for all $\vec{r}$. For any function F of the dimer configuration, let $\langle F \rangle = \mathcal{Z}_0^{-1} \sum_{\psi \in \mathcal{C}_0} F(\psi) \mathrm{e}^{-E_\psi/T}$ be the average over the ensemble $\mathcal{C}_0$ of close-packed dimer configurations, where E_ψ is the energy of configuration ψ (see below), T the temperature ($k_\mathrm{B} = 1$), and $\mathcal{Z}_0$ the partition function.

An equal-weight ensemble of all close-packed configurations (i.e., setting $E_\psi = 0$) is a Coulomb liquid, described by an emergent noncompact U(1) gauge theory [2]. Sites where $n(\vec{r}) \neq 1$ have charge $Q(\vec{r}) = (-1)^{r_x + r_y + r_z}[n(\vec{r}) - 1]$ in this description, and are hence referred to as 'monopoles'. A pair of oppositely-charged test monopoles (for example, one empty site from each sublattice) is deconfined in the liquid phase.

The model can be driven into a confining, ordered phase using an energy $-v_2 \mathcal{N}_2$, where $\mathcal{N}_2$ is the number of nearest-neighbor parallel dimers [3]. For $T \ll v_2$, the dimers form a crystal that maximizes $\mathcal{N}_2$ and breaks spatial symmetries. A corresponding order parameter is the 'magnetization density'

$$N_\mu = \frac{2}{L^3} \sum_{\vec{r}} (-1)^{r_\mu} d_\mu(\vec{r}) \,. \tag{1}$$

As T increases through a critical value T_c, there is a direct transition into the dimer liquid [3].

Here, we set $v_2 = 1$ and use a configuration energy $E_\psi = -\mathcal{N}_2 + v_4 \mathcal{N}_4$, where $\mathcal{N}_4$ is the number of cubes of the lattice that contain four parallel dimers [28]; see Fig. 1(d). For $v_4 > 0$ this is a frustrating interaction which decreases T_c. More importantly, as v_4 is varied, the order of the transition changes from clearly first order (at $v_4 < 0$) to apparently continuous ($v_4 > 0$), with an apparent tricritical point near $v_4 = 0$ [28]. This point introduces complications in the scaling analysis, which we avoid by using large positive v_4.

There is no local order parameter for the liquid, which is instead characterized by monopole deconfinement [1]. Defining operators $\varphi(\vec{r})$ and $\bar{\varphi}(\vec{r})$ that respectively decrement and increment $Q(\vec{r})$, the monopole distribution function G_m is

$$G_\mathrm{m}(\vec{r}_+, \vec{r}_-) \equiv \frac{1}{\mathcal{Z}_0} \sum_{\psi \in \mathcal{C}(\vec{r}_+, \vec{r}_-)} \mathrm{e}^{-E_\psi/T} = \langle \bar{\varphi}(\vec{r}_+) \varphi(\vec{r}_-) \rangle \,. \tag{2}$$

$\mathcal{C}(\vec{r}_+, \vec{r}_-)$ denotes the ensemble of dimer configurations that are close-packed except for a pair of monopoles of charge ± 1 at sites $\vec{r}_\pm$. In the liquid, G_m remains nonzero as $|\vec{r}_+ - \vec{r}_-| \to \infty$ (monopole deconfinement). We define global operators $\varphi = L^{-3} \sum_{\vec{r}} \varphi(\vec{r})$ and $\bar{\varphi}$.

Continuum theory An action believed to describe the transition [4–6] involves a noncompact U(1) gauge field $\vec{A}$, minimally coupled to a 2-component complex vector $\boldsymbol{z}$,

$$\mathcal{L} = \frac{\kappa}{2} |\vec{\nabla} \times \vec{A}|^2 + |(\vec{\nabla} - \mathrm{i}\vec{A})\boldsymbol{z}|^2 + s|\boldsymbol{z}|^2 + u(|\boldsymbol{z}|^2)^2 \,, \tag{3}$$

with s tuned to its critical value and $u, \kappa > 0$. In terms of this theory, referred to as NCCP^1, the local magnetization is $\vec{N} \sim \boldsymbol{z}^\dagger \vec{\boldsymbol{\sigma}} \boldsymbol{z}$ and the monopole operator $\bar{\varphi}(\vec{r})$ creates a source of the 'magnetic field' $\vec{\nabla} \times \vec{A}$. This continuum theory also describes the Néel–VBS transition in spin-$\frac{1}{2}$ antiferromagnets—where $\boldsymbol{z}^\dagger \vec{\boldsymbol{\sigma}} \boldsymbol{z}$ is the local Néel vector and φ is the VBS order parameter [7, 8]—and the 'hedgehog-free' O(3) model [29].

SO(5) *symmetry* The claim of SO(5) symmetry is that the critical point has an emergent symmetry under SO(5) rotations of the five-component order parameter

$$\Phi = (N_x, N_y, N_z, c\varphi_x, c\varphi_y) \,, \tag{4}$$

where $\varphi_x = \frac{1}{2}(\varphi + \bar{\varphi})$, $\varphi_y = \frac{1}{2\mathrm{i}}(\varphi - \bar{\varphi})$, and c is a constant. The dimer model's microscopic symmetries [30] are: lattice point group operations (rotations and reflections), which act both on the spatial coordinate and on $\vec{N}$; translation by a lattice vector $\vec{\delta}_\mu$, which changes the sign of both N_μ and φ_y; and SO(2) rotations of (φ_x, φ_y). This SO(2) [or U(1)] symmetry is equivalent to the requirement of overall monopole charge neutrality in correlators (it becomes a conventional symmetry, acting on dynamical fields in a partition sum, in a dual description). In order to demonstrate SO(5), the key step is to demonstrate an emergent symmetry that rotates $\vec{\varphi}$ into $\vec{N}$. Any symmetry operation of this type, when combined with microscopic symmetry, implies SO(5) [30]. Concretely, we test for invariance under SO(3) rotations of $\vec{N}$ and, crucially, under rotations of the two-component vector $\vec{\chi} = (N_x, c\varphi_x)$, which we denote $\mathrm{SO}(2)_\chi$. This symmetry implies full SO(5) [30].

Because φ cannot be expressed as a function of the dimer configuration [39], we cannot measure a probability distribution of χ. Instead, consider the implications of the putative $\mathrm{SO}(2)_\chi$ symmetry for moments $\langle \chi_\mu \chi_\nu \cdots \rangle$. Some relations are already guaranteed by the microscopic symmetries under $N_x \to -N_x$ and $\varphi_x \to -\varphi_x$. The first nontrivial equality is [30]

$$\langle N_x^2 \rangle = c^2 \langle \varphi_x^2 \rangle \,, \tag{5}$$

implying that $\langle N_x^2\rangle/\langle\varphi_x^2\rangle$ is independent of system size at the transition.

Defining normalized quantities $\tilde{N}_x = N_x/\langle N_x^2\rangle^{1/2}$ and $\tilde{\varphi}_x = \varphi_x/\langle\varphi_x^2\rangle^{1/2}$ with unit variance, $\mathrm{SO}(2)_\chi$ implies the three nontrivial identities

$$\langle\tilde{N}_x^4\rangle = \langle\tilde{\varphi}_x^4\rangle = 3\langle\tilde{N}_x^2\tilde{\varphi}_x^2\rangle\,, \qquad \langle\tilde{N}_x^2\tilde{\varphi}_x^4\rangle = \langle\tilde{N}_x^4\tilde{\varphi}_x^2\rangle\,. \tag{6}$$

Checking these requires sampling configurations with up to four monopoles.

Numerical algorithm Correlators containing φ and $\bar{\varphi}$ are given by

$$\left\langle F\bar{\varphi}^{m/2}\varphi^{m'/2}\right\rangle = \delta_{mm'}\frac{[(m/2)!]^2}{L^{3m}\mathcal{Z}_0}\sum_{\psi\in C_m}F(\psi)\,\mathrm{e}^{-E_\psi/T}\,, \tag{7}$$

where C_m is the set of all configurations with $\frac{m}{2}$ monopoles of each sign. In our simulations, the only allowed monopoles are empty sites, or 'monomers'. (As a result, the sum defining the global variable φ runs over only one sublattice, and that for $\bar{\varphi}$ runs over the other.) Allowing overlapping dimers would make no essential difference.

We calculate such expectation values using an extension of the standard worm algorithm [31–33]. At each iteration, we either construct a worm, giving a new configuration with the same monomer number m, or apply a monopole–number–changing update. If $m = 0$, the latter attempts to remove a dimer, leaving behind two neighboring monopoles of opposite charge. If $m = 4$, we attempt to add a dimer, annihilating two monopoles. If $m = 2$, either addition or removal is attempted, with fixed relative probability. The location for the attempted move is chosen randomly and the update is accepted with the standard Metropolis probability for its energy change.

This procedure effectively samples from the partition sum

$$\mathcal{Z}_{\mathrm{eff}} = \sum_{m\in\{0,2,4\}} f_m \sum_{\psi\in C_m}\mathrm{e}^{-E_\psi/T}\,, \tag{8}$$

with weights f_m determined by the probabilities used at each step (chosen to optimize the algorithm [30]). Comparison with Eq. (7) relates the desired quantities to expectation values in this ensemble, conditioned on m. Restricting to $m \le 4$ allows us to calculate quantities with up to four φ operators, including those in Eqs. (5, 6). The algorithm extends straightforwardly to larger m, allowing higher moments to be calculated, but at increasing computational cost.

Results We first verify SO(3) symmetry of $\vec{N}$ at the critical point for $v_4 = 10$, extending the results of Ref. [34] at $v_4 = 0$. Figure 2(a) shows a cross section (with $N_z = 0$ [40]) through the probability distribution for $\vec{N}$ at the critical temperature T_c. (T_c is determined using the procedure described below.) The circular distribution indicates that the microscopic symmetry under 90° rotations of $\vec{N}$ is enhanced to continuous symmetry at criticality. For a quantitative measure of this emergent symmetry, Fig. 2(b) shows the ratio $6\langle N_x^2N_y^2\rangle/\langle N_x^4+N_y^4\rangle$ versus L, at T_c. This ratio approaches unity as L increases, indicating (at least) an emergent rotation

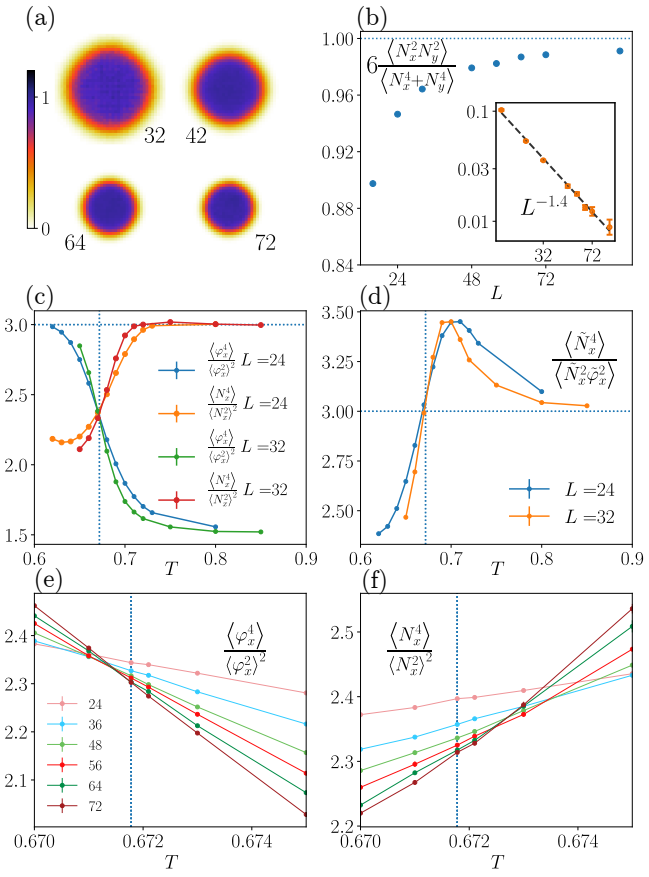

FIG. 2. Monte Carlo results across the columnar ordering transition (with $v_4 = 10$). (a) Cross section, with $N_z = 0$, through the magnetization density distribution at the critical temperature T_c [determined in Fig. 3(a)], labeled by system size L. (b) Ratio of moments $6\langle N_x^2N_y^2\rangle/\langle N_x^4+N_y^4\rangle$, equal to unity in the case of SO(3) symmetry, plotted as a function of L at $T = T_c$. Inset: absolute difference between this ratio and unity, on a double-logarithmic scale, along with a power-law fit. (c) Binder cumulants of magnetization and monopole operator, over a broad temperature range. Dotted vertical line (this and subsequent panels) shows T_c. (d) Normalized cumulant ratio $\langle\tilde{N}_x^4\rangle/\langle\tilde{N}_x^2\tilde{\varphi}_x^2\rangle$, which equals 3 when SO(5) is present. (e,f) Binder cumulants close to T_c.

symmetry of order greater than 4 [30]. We argue this provides strong evidence of continuous SO(3) symmetry.

We now turn to quantities that test for symmetry mixing $\vec{N}$ and φ, focusing on $v_4 = 10$. We consider comoments of N_x and φ_x (their joint distribution is not directly measurable as φ is not a function of the dimer configuration [39]).

The two Binder cumulants $\langle N_x^4\rangle/\langle N_x^2\rangle^2$ and $\langle\varphi_x^4\rangle/\langle\varphi_x^2\rangle^2$ are shown in Fig. 2(c) over a broad temperature range. Both take the expected values deep within the two phases [30] and cross at approximately the same temperature, consistent with a continuous phase transition directly between dimer crystal and liquid. The first hint of SO(5) symmetry is that the two Binder cumulants take the same value at their crossing points. It should be noted that this value is not what one would expect for a Gaussian probability distribution (*viz* 3),

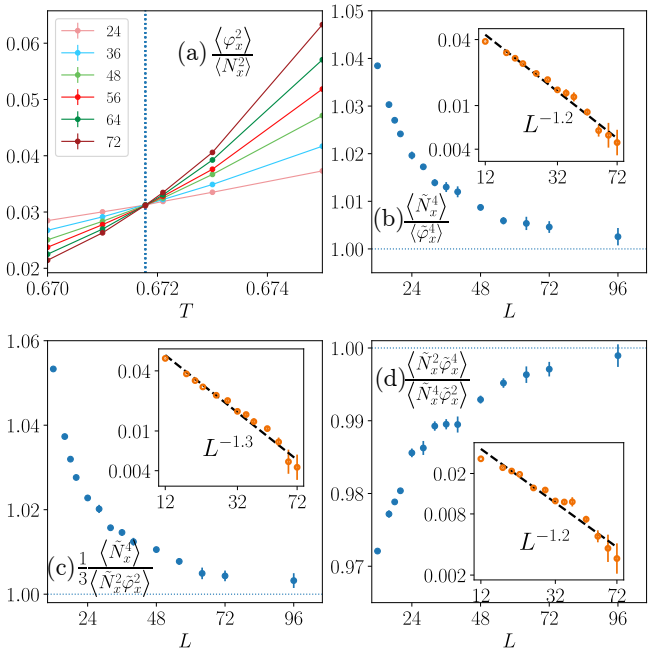

FIG. 3. Monte Carlo results demonstrating SO(5) symmetry at the transition (again $v_4 = 10$). (a) Ratio $\langle\varphi_x^2\rangle/\langle N_x^2\rangle$ of variances. The temperature of the crossing (vertical dashed line) yields our estimate of T_c. (b–d) Ratios of cumulants, each constrained to unity by SO(5). In each panel, the inset shows a log–log plot of the absolute difference of the ratio from unity versus L, with a best-fit power law.

which would provide a trivial explanation for our SO(5) results. Next, Figure 2(d) shows, for the same temperature range, $\langle\tilde{N}_x^4\rangle/\langle\tilde{N}_x^2\tilde{\varphi}_x^2\rangle$, an example of a ratio constrained by SO(5) [Eq. (6)]. The ratio indeed takes the expected value of 3 at T_c, as we show to much higher precision below, while approaching the expected limits in both phases.

Zooming in on the critical region, Fig. 2(e,f) shows the above Binder cumulants for N_x and φ_x in the neighborhood of their crossing points. As noted in previous studies of this transition [28, 33], the crossings drift significantly with L, and the respective crossing temperatures for the two Binder cumulants differ by a relative amount of order 10^{-3}.

However, the quantity $\langle\varphi_x^2\rangle/\langle N_x^2\rangle$ has a remarkably sharp crossing at a temperature in between the two: see Fig. 3(a). This crossing is a consequence of SO(5) symmetry [and determines the constant c in Eq. (5)]. Since this crossing point is much better-defined than that of the Binder cumulants, we use it as our best estimate of the critical temperature, giving $T_c = 0.6718(1)$ for $v_4 = 10$.

To quantify the precision of SO(5), we show the ratios $\langle\tilde{N}_x^4\rangle/\langle\tilde{\varphi}_x^4\rangle$, $\frac{1}{3}\langle\tilde{N}_x^4\rangle/\langle\tilde{N}_x^2\tilde{\varphi}_x^2\rangle$, and $\langle\tilde{N}_x^2\tilde{\varphi}_x^4\rangle/\langle\tilde{N}_x^4\tilde{\varphi}_x^2\rangle$, evaluated at this temperature, in Fig. 3(b–d). All three approach unity, as expected from SO(5) [Eq. (6)]. The corrections are small in magnitude and decrease approximately as power laws, $\sim L^{-|y_{\rm irr}|}$, over the full range of L studied. The effective irrelevant exponent $y_{\rm irr}$ is consistent with that observed for the corrections to the SO(3) symmetry of $\vec{N}$ [see Fig. 2(b), inset].

We show results for the transition at smaller v_4 in the Supplemental Material [30]. (Recall that there is a critical line in the plane of the frustrating interaction v_4 and temperature, with $v_4 \simeq 0$ previously identified as separating continuous and first-order transitions [28].) Importantly, results for $v_4 = 1$ are similar to $v_4 = 10$: the ratios approach their SO(5)-invariant values to a similar level of precision at the largest sizes. Results at $v_4 = 0.2$ are still consistent with emergent SO(5), while at $v_4 = 0$, close to the apparent tricritical point, the deviation from unity is considerably larger at the largest sizes. Even here, SO(5) may improve at still larger sizes, but see Discussion for another explanation.

We expect that corrections to SO(5) arise from perturbations to a hypothetical SO(5)-invariant continuum action that are effectively irrelevant at least on the scales we access. If the critical properties are only 'quasiuniversal', this SO(5)-invariant action is not that of an RG fixed point, but instead associated with a relatively well-defined SO(5)-invariant flow line. Classifying operators into SO(5) representations, the simplest possibility is that the leading perturbations arise from a symmetric tensor X_{abcd} [20, 23, 41]. Microscopic dimer model symmetries allow as perturbations: higher-order asymmetry between φ and $\vec{N}$, $\sum_{a,b=1}^{3} X_{aabb}$; and cubic anisotropy for $\vec{N}$, $\sum_{a=1}^{3} X_{aaaa}$. The consistency of $y_{\rm irr}$ estimates (between -1.4 and -1.2) for distinct ratios at $v_4 = 10$ accords with this picture. For $v_4 = 1$ we obtain slightly larger values (between -1.7 and -1.4), while in the loop model a rough estimate gave $y_{\rm irr} \sim -0.8$. In the 'quasiuniversal' picture $y_{\rm irr}$ is an effective exponent which drifts as a function of L/L_0 with nonuniversal L_0; such drifts may explain the differences in $y_{\rm irr}$.

Discussion We have presented evidence for SO(5) symmetry at the ordering transition in the cubic dimer model, which is at least as robust as critical scaling. This is an unusual example of emergent symmetry in a purely classical model, relating the magnetization $\vec{N}$ to the monopole operator φ.

Because φ is not a local observable in terms of the dimers, it is not possible to measure its distribution function. We have instead used identities between comoments to demonstrate a symmetry rotating $\vec{\varphi}$ into $\vec{N}$. Together with microscopic symmetry, this implies full SO(5).

These results show that very precise SO(5) is a robust property of a large class of models described by NCCP^1. Still, it is possible that NCCP^1 does not have a true critical point, but instead only 'quasiuniversal' properties arising from a near-vanishing of the beta function [19, 23]. The 'critical' properties are then associated with an approximate convergence of the flows to an SO(5)-invariant flow line, and SO(5) symmetry is approximate rather than exact [42]. Our results are compatible with this scenario, although over the scales we have studied SO(5) resembles an exact symmetry of the IR theory, whose precision improves with L.

This scenario allows a sharp crossover, as a function of a microscopic coupling, between a regime where the transition is apparently continuous (very weakly first-order) and one where it is strongly first-order. The 'tricritical' point $v_4 \simeq 0$ might in

fact be such a crossover. If so, an analysis of the SO(5) ratios for $v_4 \sim 0$ could give useful insight into the RG flows. Another extension would be to reduce the lattice symmetry of the model so only 4 of the 6 ordered states remain [6]. This would yield a platform for investigating the possibility of emergent O(4) symmetry in the 'easy-plane' version of NCCP[1] [23, 35, 36].

We thank J. T. Chalker for useful discussions. This work was supported by EPSRC Grant No. EP/M019691/1 (SP) and Grant No. EP/N028678/1 (AN). We thank MPI-PKS Dresden and NPSF-CDAC Pune for providing computing resources.

[1] D. A. Huse, W. Krauth, R. Moessner, and S. Sondhi, *Coulomb and liquid dimer models in three dimensions*, Phys. Rev. Lett. **91**, 167004 (2003).
[2] C. L. Henley, *The "Coulomb phase" in frustrated systems*, Annu. Rev. Cond. Matt. Phys. **1**, 179 (2010).
[3] F. Alet, G. Misguich, V. Pasquier, R. Moessner, and J. L. Jacobsen, *Unconventional Continuous Phase Transition in a Three-Dimensional Dimer Model*, Phys. Rev. Lett. **97**, 030403 (2006).
[4] S. Powell and J. T. Chalker, SU(2)-*Invariant Continuum Theory for an Unconventional Phase Transition in a Three-Dimensional Classical Dimer Model*, Phys. Rev. Lett. **101**, 155702 (2008); *Classical to quantum mapping for an unconventional phase transition in a three-dimensional classical dimer model*, Phys. Rev. B **80**, 134413 (2009).
[5] D. Charrier, F. Alet, and P. Pujol, *Gauge Theory Picture of an Ordering Transition in a Dimer Model*, Phys. Rev. Lett. **101**, 167205 (2008).
[6] G. Chen, J. Gukelberger, S. Trebst, F. Alet, and L. Balents, *Coulomb gas transitions in three-dimensional classical dimer models*, Phys. Rev. B **80**, 045112 (2009).
[7] T. Senthil, A. Vishwanath, L. Balents, S. Sachdev, and M. P. A. Fisher, *Deconfined Quantum Critical Points*, Science **303**, 1490 (2004).
[8] T. Senthil, L. Balents, S. Sachdev, A. Vishwanath, and M. P. A. Fisher, *Quantum criticality beyond the Landau-Ginzburg-Wilson paradigm*, Phys. Rev. B **70**, 144407 (2004).
[9] A. W. Sandvik, *Evidence for Deconfined Quantum Criticality in a Two-Dimensional Heisenberg Model with Four-Spin Interactions*, Phys. Rev. Lett. **98**, 227202 (2007).
[10] R. G. Melko and R. K. Kaul, *Scaling in the fan of an unconventional quantum critical point*, Phys. Rev. Lett. **100**, 017203 (2008),
[11] A. B. Kuklov, M. Matsumoto, N. V. Prokof'ev, B. V. Svistunov, and M. Troyer, *Deconfined criticlaity: generic first-order transition in the $SU(2)$ symmetry case*, Phys. Rev. Lett. **101**, 050405 (2008)
[12] F.-J. Jiang, M. Nyfeler, S. Chandrasekharan, and U.-J. Wiese, *From an antiferromagnet to a valence bond solid: evidence for a first-order phase transition*, Journal of Statistical Mechanics: Theory and Experiment **2008**, P02009 (2008)
[13] J. Lou, A. W. Sandvik, and N. Kawashima, *Antiferromagnetic to valence-bond-solid transitions in two-dimensional $SU(N)$ Heisenberg models with multispin interactions*, Phys. Rev. B **80**, 180414 (2009)
[14] A. Banerjee, K. Damle, and F. Alet, *Impurity spin texture at a deconfined quantum critical point*, Phys. Rev. B **82**, 155139 (2010)
[15] A. W. Sandvik, *Continuous Quantum Phase Transition between an Antiferromagnet and a Valence-Bond Solid in Two Dimensions: Evidence for Logarithmic Corrections to Scaling*, Phys. Rev. Lett. **104**, 177201 (2010).
[16] K. Harada, T. Suzuki, T. Okubo, H. Matsuo, J. Lou, H. Watanabe, S. Todo, and N. Kawashima, *Possibility of deconfined criticality in $SU(N)$ Heisenberg models at small N*, Phys. Rev. B **88**, 220408 (2013)
[17] K. Chen, Y. Huang, Y. Deng, A. B. Kuklov, N. V. Prokof'ev, and B. V. Svistunov, *Deconfined Criticality Flow in the Heisenberg Model with Ring-Exchange Interactions*, Phys. Rev. Lett. **110**, 185701 (2013).
[18] H. Shao, W. Guo, and A. W. Sandvik, *Quantum criticality with two length scales*, Science **352**, 213 (2016)
[19] A. Nahum, P. Serna, J. T. Chalker, M. Ortuño, and A. M. Somoza, *Deconfined Quantum Criticality, Scaling Violations, and Classical Loop Models*, Phys. Rev. X **5**, 041048 (2015).
[20] A. Nahum, P. Serna, J. T. Chalker, M. Ortuño, and A. M. Somoza, *Emergent* SO(5) *symmetry at the Néel to valence-bond-solid transition*, Phys. Rev. Lett. **115**, 267203 (2015).
[21] A. Tanaka and X. Hu, *Many-Body Spin Berry Phases Emerging from the π-Flux State: Competition between Antiferromagnetism and the Valence-Bond-Solid State*, Phys. Rev. Lett. **95**, 036402 (2005).
[22] T. Senthil and M. P. A. Fisher, *Competing orders, nonlinear sigma models, and topological terms in quantum magnets*, Phys. Rev. B **74**, 064405 (2006).
[23] C. Wang, A. Nahum, M. A. Metlitski, C. Xu, and T. Senthil, *Deconfined Quantum Critical Points: Symmetries and Dualities*, Phys. Rev. X **7**, 031051 (2017).
[24] H. Suwa, A. Sen, and A. W. Sandvik, *Level spectroscopy in a two-dimensional quantum magnet: Linearly dispersing spinons at the deconfined quantum critical point*, Phys. Rev. B **94**, 144416 (2016).
[25] L. Bartosch, *Corrections to scaling in the critical theory of deconfined criticality*, Phys. Rev. B **88**, 195140 (2013)
[26] D. Simmons-Duffin, unpublished.
[27] Y. Nakayama and T. Ohtsuki, *Necessary condition for emergent symmetry from the conformal bootstrap*, Phys. Rev. Lett. **117**, 131601 (2016)
[28] D. Charrier and F. Alet, *Phase diagram of an extended classical dimer model*, Phys. Rev. B **82**, 014429 (2010).
[29] O. I. Motrunich and A. Vishwanath, *Emergent photons and transitions in the O(3) sigma model with hedgehog suppression*, Phys. Rev. B **70**, 075104 (2004)
[30] See Supplemental Material.
[31] N. Prokof'ev and B. Svistunov, *Worm algorithms for classical statistical models*, Phys. Rev. Lett. **87**, 160601 (2001)
[32] A. W. Sandvik and R. Moessner, *Correlations and confinement in nonplanar two-dimensional dimer models*, Phys. Rev. B **73**, 144504 (2006).
[33] G. J. Sreejith and S. Powell, *Critical behavior in the cubic dimer model at nonzero monomer density*, Phys. Rev. B **89**, 014404 (2014).
[34] G. Misguich, V. Pasquier, and F. Alet, *Correlations and order parameter at a Coulomb-crystal phase transition in a three-dimensional dimer model*, Phys. Rev. B **78**, 100402(R) (2008).
[35] Y. Q. Qin, Y.-Y. He, Y.-Z. You, Z.-Y. Lu, A. Sen, A. W. Sandvik, C. Xu, and Z. Y. Meng, *Duality between the deconfined quantum critical point and the bosonic topological transition*, Phys. Rev. X **7**, 031052 (2017)
[36] X.-F. Zhang, Y.-C. He, S. Eggert, R. Moessner, and F. Pollmann, *Continuous easy-plane deconfined phase transition on the kagome lattice*, Phys. Rev. Lett. **120**, 115702 (2018)
[37] P. Serna and A. Nahum, *Emergence and spontaneous breaking of approximate* O(4) *symmetry at a weakly first-order deconfined phase transition*, arXiv:1805.03759 (2018).
[38] More formally, emergent SO(5) is consistent with the anomaly

structure of NCCP[1] [23].
[39] We can measure the joint distribution of three components (N_x, N_y, N_z) of Φ, but not all five. The loop model also allows measuring the joint distribution for at most three order parameter components: two VBS and one Néel. The imaginary (topological) term in the sigma model [21, 22] indicates at most 3 components can be local 'diagonal' observables (functions of configuration) in any sign-free representation of this universality class.
[40] In fact $|N_z| < 0.00625$ (half-width of one pixel).
[41] $X_{abcd} \sim \Phi_a\Phi_b\Phi_c\Phi_d - (\ldots)$, with $\sum_{a=1}^{5} X_{aacd} = 0$.
[42] At still larger scales (beyond pseudocritical regime) this likely yields a regime with approximate SO(5) Goldstone modes [23, 37].